Published in final edited form as:
Oncogene. 2009 January 15; 28(2): 219–230. doi:10.1038/onc.2008.379.

Rbpj conditional knockout reveals distinct functions of Notch4/Int3 in mammary gland development and tumorigenesis

A Raafat[1], **S Lawson**[1], **S Bargo**[1], **M Klauzinska**[1], **L Strizzi**[1], **AS Goldhar**[1], **K Buono**[2], **D Salomon**[1], **BK Vonderhaar**[1], and **R Callahan**[1]

[1] Mammary Biology and Tumorigenesis Laboratory, National Cancer Institute, National Institutes of Health, Bethesda, MD, USA

[2] Laboratory of Genetics and Physiology, National Institute of Diabetes and Digestive and Kidney Diseases, National Institutes of Health, Bethesda, MD, USA

Abstract

Transgenic mice expressing the Notch 4 intracellular domain (ICD) (Int3) in the mammary gland have two phenotypes: arrest of mammary alveolar/lobular development and mammary tumorigenesis. *Notch4* signaling is mediated primarily through the interaction of Int3 with the transcription repressor/activator Rbpj. We have conditionally ablated the *Rbpj* gene in the mammary glands of mice expressing whey acidic protein (Wap)-*Int3*. Interestingly, *Rbpj* knockout mice (Wap-Cre^{+}/$Rbpj^{-/-}$/ Wap-*Int3*) have normal mammary gland development, suggesting that the effect of endogenous *Notch* signaling on mammary gland development is complete by day 15 of pregnancy. RBP-J heterozygous (Wap-Cre^{+}/$Rbpj^{-/+}$/ Wap-*Int3*) and *Rbpj* control ($Rbpj^{flox/flox}$/Wap-*Int3*) mice are phenotypically the same as Wap-*Int3* mice with respect to mammary gland development and tumorigenesis. In addition, the Wap-Cre^{+}/$Rbpj^{-/-}$/Wap-*Int3*-knockout mice also developed mammary tumors at a frequency similar to *Rbpj* heterozygous and Wap-*Int3* control mice but with a slightly longer latency. Thus, the effect on mammary gland development is dependent on the interaction of the Notch ICD with the transcription repressor/activator Rbpj, and *Notch*-induced mammary tumor development is independent of this interaction.

Keywords

RBP-J; Int3; tumorigenesis

Introduction

The *Notch* signaling pathway is an evolutionarily conserved intercellular signaling mechanism (reviewed by Callahan and Egan, 2004). Genes of the *Notch* family encode transmembrane receptors that interact with membrane-bound ligands encoded by the *Delta/Serrate/ Jagged* gene families. The signal induced by ligand binding is transmitted by a process involving proteolytic cleavage of the receptor by γ-secretase followed by nuclear translocation of the Notch intracellular domain (ICD). The Notch ICD translocates to the nucleus and serves as a transcription activator. The Notch ICD does not possess DNA binding activity; rather it associates with the transcription factor Rbpj, the primary transcriptional mediator of canonical *Notch* signaling. The Notch-ICD–*Rbpj* complex transactivates promoters containing Rbpj-binding sites (Kato *et al*., 1996).

Correspondence: Dr R Callahan, Mammary Biology and Tumorigenesis Laboratory, National Cancer Institute, National Institutes of Health, 37 Convent Drive, Building 37, Room 1118A, Bethesda, MD 20892, USA. rc54d@nih.gov.

Evidence for a link between Notch signaling and mammary tumorigenesis came from observations that integration of the mouse mammary tumor virus (MMTV) into the *Notch4* gene leads to the formation of mammary tumors (Gallahan and Callahan, 1987). MMTV integration into *Notch4* results in the transcription of a truncated *Notch4* mRNA species (designated as *Int3*) that represents a gain-of-function mutation (Robbins *et al*., 1992; Kordon *et al*., 1995; Gallahan and Callahan, 1997; Raafat *et al*., 2004). Expression of *Int3* under control of mammary-specific regulatory elements in transgenic mice confirmed that activation of *Notch* signaling leads to the establishment of mammary tumors in 100% of female mice (Jhappan *et al*., 1992; Gallahan *et al*., 1996). Expression of *Int3* as a transgene from the whey acidic protein (Wap) promoter or the MMTV-Long terminal repeat (LTR) in transgenic mice blocks normal mammary lobular development and the ability of these females to lactate (Jhappan *et al*., 1992; Smith *et al*., 1995; Gallahan *et al*., 1996). Wap- and MMTV-Int3 mice develop mammary tumors with 100% penetrance in breeding and nulliparous females (Jhappan *et al*., 1992; Smith *et al*., 1995; Gallahan *et al*., 1996).

A variant *Int3* RNA species was detected in certain human tumor cell lines and was designated as *h-Int3sh* (Imatani and Callahan, 2000). *Int3sh* is missing sequences encoding the Rbpj-binding region (RAM23) of the Notch4 ICD. We have shown that *h-Int3sh* can still activate transcription from the *Hes1* promoter, although at a reduced efficiency (Raafat *et al*., 2004). Interestingly, mammary gland development in transgenic mice overexpressing *h-Int3sh* under the control of Wap promoter (Wap-*h-Int3sh*) appears normal and the females lactate (Raafat *et al*., 2004). However, multiparous Wap-*h-Int3sh* females develop mammary tumors. These results are compatible with the concept of a gradient in *Notch4* signaling affecting mammary gland development and tumorigenesis. In this model, impairment of mammary gland development requires high levels of Notch signaling, whereas induction of mammary tumors by activated *Notch4* would require lower levels of Notch signaling. The aim of this study was to investigate, *in vivo*, the biological role of *Int3-Rbpj*-dependent and *Int3-Rbpj*-independent signaling pathways in mammary gland development and tumorigenesis.

Results

Inactivation of *Rbpj* and mammary gland development

The MMTV LTR-*Int3* and Wap-*Int3* transgenic mice exhibit two phenotypes with 100% penetrance: lack of mammary alveolar/lobular development and mammary tumor development, respectively (Jhappan *et al*., 1992; Gallahan *et al*., 1996). To determine whether these phenotypes are a consequence of a canonical *Int3*/*Rbpj* signaling pathway, we conditionally deleted exons 6 and 7 of the *Rbpj* gene in the presence of the mammary gland-specific Wap-*Cre* transgene (Figure 1a). Exons 6 and 7 encode the DNA-binding and Notch-binding domains, and loss of these exons results in the complete loss of *Rbpj*-mediated *Notch* signaling (Han *et al*., 2002). In addition, RT–PCR analysis of total RNA extracted from three independent tumors of *Rbpj* knockout and *Rbpj* control mice showed that only the *Rbpj* knockout tumor RNAs are negative for neomycin phoshotransferase (*Neo*) RNA (Figure 1b). Through a series of genetic crosses between Wap-*Cre*, $Rbpj^{flox/flox}$ and Wap- *Int3* mice, female mice with the following genotypes were obtained: Wap-Cre^{+}/$Rbpj^{-/-}$/Wap-*Int3* (Wap-*Int3*/*Rbpj* knockout); Wap-Cre^{+}/$Rbpj^{-/+}$/Wap-*Int3* (Wap- *Int3*/*Rbpj* heterozygous); and $Rbpj^{flox/flox}$/ Wap-*Int3* (Wap-*Int3*/*Rbpj* control) (see Materials and Methods). Interestingly, the Wap-Cre^{+}/$Rbpj^{-/-}$ females that were used in the generation of the *Rbpj* knockout mice had no detectable phenotype with regard to mammary gland development. This suggests that the contribution of endogenous *Notch*/*Rbpj* signaling to mammary alveolar/ lobular development is completed before the expression of the Wap-*Cre* transgene.

The functional unit in the mammary gland during lactation is the alveolus, which produces and secretes milk. In the normal mammary gland, the lobules and their alveoli start to expand at

day 5 of pregnancy (Oakes *et al*., 2006) and continue their growth and differentiation during gestation to form functionally active glandular structures that secrete milk proteins. However, as shown in Figure 2 and earlier (Gallahan *et al*., 1996), by day 1 of lactation, expression of Wap-*Int3* in Wap-*Int3*/*Rbpj* control mice exhibits an impaired ability to form functionally competent alveolar/lobular structures as observed in whole mounts and histological sections of mammary glands (panels a and e, respectively) as compared with normal lactating wild-type FVB/N mammary glands (panels d and h, respectively). Similarly, alveolar/lobular development in mammary glands from day 1 lactating Wap-*Int3*/*Rbpj* heterozygous mice are inhibited to a similar degree, as these females are unable to nurse their pups (Figures 2b and f, respectively). To determine whether the lack of alveolar/ lobular development in the mammary glands of Wap-*Int3*/*Rbpj* heterozygous and Wap-*Int3*/*Rbpj* control mice was also reflected in milk composition, β-casein levels were measured by immunohistochemistry (IHC) (Figure 2). β-Casein production was high in the FVB/N mammary gland (Figure 2l) and not detectable in the mammary glands of Wap-*Int3*/*Rbpj* heterozygous (panel j) and Wap-*Int3*/*Rbpj* control mice (panel i).

The effects of Wap-*Int3* expression on mammary gland development are not manifested in Wap-*Int3*/*Rbpj* knockout females. The morphology of the mammary gland (in the whole mount and histology section Figure 2c and g, respectfully) from day1 lactating females is very similar to the normal FVB/N mammary gland, and β-casein can be detected in the alveolar/lobular structures (Figure 2k). In addition, the Wap-*Int3*/*Rbpj* knockout females can successfully nurse their pups.

Mammary tumorigenesis is independent of *Rbpj* function

Morphological analysis of mammary glands revealed the presence of focal hyperproliferative lesions arising within the mammary ducts of Wap-*Int3*/*Rbpj* knockout, Wap-*Int3*/*Rbpj* heterozygous and Wap-*Int3*/*Rbpj* control females (Figure 3a). Irrespective of the genotype, the number of the lesions averaged 24 per gland (Figure 3b). By the second pregnancy, 80% of the Wap-*Int3*/*Rbpj* heterozygous and Wap-*Int3*/*Rbpj* control mice developed mammary tumors (Figure 3c). However, tumor-free survival was longer in the Wap-*Int3*/*Rbpj* knockout females: 80% of them developed tumors after three or four pregnancies. Thus, although the loss of *Rbpj* function seems to have no effect on Int3-induced mammary tumorigenesis, it may affect the rate of tumor cell proliferation.

Histological analysis of the primary mammary tumors showed that they are primarily solid (Figures 3d–f) or papillary mammary adenocarcinomas (Figures 3g–i). The solid tumors from Wap-*Int3*/*Rbpj* knockout (panel 3d), Wap-*Int3*/*Rbpj* heterozygous (panel 3e) and Wap-*Int3*/*Rbpj* control (panel 3f) mice consist mostly of tightly packed, eosinophilic epithelial tumor cells. Rare mitotic figures can be identified. In the papillary adenocarcinoma from a Wap-*Int3*/*Rbpj*-knockout (panel 3g) mouse, papillary structures project toward a lumen containing eosinophilic material and numerous apoptotic bodies and consist predominantly of a monolayer of tumor epithelial cells lining an identifiable stromal axis (arrows). The papillary structures shown in Figure 3h (arrows) in a Wap-*Int3*/*Rbpj* heterozygous tumor are irregular and consist of hyperchromic cells with areas of more florid proliferation. The stromal axis is not as evident within the papillary formations. Streams of dense connective cells can be identified surrounding the papillary lesion. In the Wap-*Int3*/*Rbpj* control tumor shown in Figure 3i, the papillary formations are smaller and less numerous (arrows) and are mixed with microglandular structures. Epithelial tumor cells are more tightly packed and regular in shape and size and the stromal component is less evident.

To confirm the malignant nature of the Wap-*Int3*/ *Rbpj* knockout tumors, fragments of nine independent tumors were transplanted bilaterally into the mammary glands of nine female nude mice. These were compared with three independent Wap-*Int3*/*Rbpj* control tumors transplanted

into six mammary glands in nude mice. Transplantation of both Wap-*Int3*/*Rbpj* knockout and control tumors was 100% successful (data not shown). The transplanted Wap-Int3/*Rbpj* knockout tumors had a latency of 8 weeks, whereas the control tumors were detectable at 5 weeks of transplantation.

Molecular consequences of *Rbpj* inactivation in Wap-Int3/*Rbpj* knockout mammary tumors

The conditional knockout of $Rbpj^{flox/flox}$ has two molecular consequences: the loss of the *Neo* gene inserted between the lox sites located in intron 5 and intron 7 and the creation of a frame shift in the open reading frame of *Rbpj* exon 8 leading to the expression of a truncated Rbpj protein (Han *et al*., 2002). To ascertain the extent to which *Rbpj* was knocked out in mammary hyperplasia and primary and transplanted Wap-Int3/*Rbpj* knockout tumors, sections of each were analysed by IHC for Neo (Figures 4A, a–f) and *Rbpj* (Figures 4B, a and b). There were virtually no cells expressing Neo in the Wap-*Int3*/*Rbpj* knockout hyperplasia (panel 4Aa), primary (panel 4Ac) or transplanted (panel 4Ae) tumors. In contrast, each of the corresponding tissues from Wap-*Int3*/*Rbpj* control mice stained positive for Neo (panels 4Ab, d and f, respectively). These results were quantified as shown in Figures 4Ag–i and demonstrate that Neo was virtually undetectable in the Wap-*Int3*/*Rbpj* knockout tissue. This conclusion was confirmed using an antibody that reacts with the C′ terminus of Rbpj and therefore should only react with wild type Rbpj. As shown in Figure 4Ba, the vast majority of Wap-*Int3*/*Rbpj* knockout tumor cells were not expressing full-length or wild-type Rbpj whereas in the Wap-*Int3*/*Rbpj* control tumor (Figure 4Bb), the tumor cells were stained and easily quantified (Figure 4Bc).

Int3 does not activate the expression of *Hes1* or *Hey2* in the absence of Rbpj

At a molecular level, the loss of active Rbpj should result in a loss of expression of the canonical Rbpj target genes such as *Hes1* or *Hey2*. Therefore, we have stained sections of Wap-*Int3*/*Rbpj* knockout andWap-*Int3*/*Rbpj* control mammary hyperplasias and primary and transplanted mammary tumors with Hes1 (Figure 5A, compare a, c and e with b, d and f, respectively) or Hey2 antibodies (compare Figure 5Ba and b). The number of cells staining positive for Hes1 (Figures 5Ag–i) and Hey2 (Figures 5Bc) was quantified. In the hyperplasia and primary tumors, there was virtually no Hes1- or Hey2-staining cells in the knockout tissue. The cells that were stained for Hes1 in the transplanted tumor may correspond to infiltrating host vasculature and epithelium. Taken together, these results are consistent with the concept that the growth of *Int3*-induced tumors is independent of *Notch*/*Rbpj* signaling, but does not formally exclude the possibility that *Rbpj*-dependent signaling is necessary for the initiation of tumorigenesis.

Cell proliferation and apoptosis in WAP-*Int3*/*Rbpj* control and knockout tumors

We examined the effects of *Rbpj* deletion on cell proliferation (Figure 6a–c) and apoptosis (Figure 6d–f) of the Wap-*Int3* tumors. *Rbpj* deletion did not result in a significant difference in the level of cell proliferation between control and knockout mice (Figure 6c). However, the level of apoptosis is significantly higher in the *Rbpj* control tumors than in the *Rbpj* knockout tumors (Figure 6f).

The effect of *Rbpj* knockout on anchorage-independent growth in soft agar by HC11 and HC11-*Int3* mammary epithelial cells

It is possible that Notch ICD may function in two ways as a regulator of transcription. Notch ICD can displace the corepressors from Rbpj and this by itself may be sufficient to indirectly activate the expression of target genes that are independent of a Notch/Rbpj interaction. This has been referred to as a $Notch^{ICD}$ permissive signaling pathway (Furriols and Bray, 2001). Alternatively, the Notch ICD may be required not only to alleviate repression by Rbpj, but also

to activate the expression of *Notch* target genes (Furriols and Bray, 2000, 2001; Bray and Furriols, 2001). We therefore have developed HC11 and HC11-*Int3* cell lines that were stably infected with *Rbpj* short hairpin RNA (shRNA) expression vectors. A reverse transcriptase PCR assay of *Rbpj* RNA expression in these cells is shown in Figure 7a. Compared with HC11 cells (lane1) or HC11 cells with a scrambled vector (lane 2), *Rbpj* RNA is virtually undetectable in HC11 cells expressing either H5 *Rbpj* shRNA (lane 3) or H6 *Rbpj* shRNA (lane 4). Similarly, compared with HC11-*Int3* (lane 5) or HC11- Int3 with the scrambled vector, HC11-*Int3*-H5 *Rbpj* shRNA (lane 7) or HC11-*Int3*-H6 *Rbpj* shRNA (lane 8) exhibited a loss or a significant decrease in the levels of *Rbpj* RNA. To validate the biological effect of *Rbpj* shRNA on *Notch*-*Rbpj*-dependent signaling, we quantified *Hey2* mRNA in HC-11-*Int3* (Figure 7b, lane 4) and HC11-*Int3*- *Rbpj* H6 shRNA (Figure 7b, lane 5). Clearly, *Rbpj* H6shRNA inhibits *Notch* canonical signaling. This inhibition did not affect cell proliferation (Figure 7c), suggesting that cell proliferation is *Rbpj* independent.

The capability for anchorage-independent growth by tissue culture cells in soft agar is accepted as a measure of their tumor-inducing potential. We have shown previously (Robbins *et al*., 1992) and in Figure 7d (lane 1) that the HC11 mouse mammary epithelial cells cannot grow in soft agar, whereas HC11-*Int3* cells do have this capability (Figure 7d, lane2). If *Notch*^{ICD} permissive signaling confers on HC11 cells the ability to grow in soft agar, then HC11 cells that are stably expressing *Rbpj* shRNA should exhibit this phenotype. To test this possibility, we compared HC11 cells expressing the *Rbpj* H6shRNA (lane 4) seeded at 15 000 cells per plate for their capacity to grow in soft agar with HC11 (lane 3) or HC11-*Int3* (lane 5) cells with the scrambled vector. HC11 cells that were stably expressing *Rbpj* shRNA do not grow in soft agar (lane 4). Alternatively, if the Int3/*Rbpj* complex is required to confer the capability for the anchorage-independent growth of HC11-*Int3* cells, then the stable expression of *Rbpj* shRNA should block growth in soft agar of these cells. However, as shown in Figure 7e, expression of *Rbpj* H6shRNA does not diminish the capability of HC11-*Int3* cells (lane 4) for anchorage-independent growth in soft agar compared with HC11- *Int3* (lane 2) or HC11-*Int3* with the scrambled vector (lane 3). These results are compatible with the conclusion that the ability of HC11-*Int3* cells for anchorage-independent growth in soft agar is independent of an *Int3*/*Rbpj* signaling pathway.

Discussion

Effect of *Rbpj* knockout on mammary gland development

Buono *et al*. (2006) have previously shown that the default developmental pathway in the mammary gland upon deletion of *Rbpj* in MMTV LTR-*Cre*/*Rbpj*$^{fl/fl}$ females results in the formation of basal cell populations and an absence of alveolar structures. Transplantation of mammary tissue from these mice demonstrated that development of the ductal tree was normal, suggesting that *Rbpj* is not necessary for the establishment of this structure. In contrast, mammary gland development occurs normally in Wap-*Cre*/*Rbpj*$^{fl/fl}$ females and they can nurse their pups. Expression from the MMTV LTR begins early during mammary gland development, whereas expression from the Wap promoter peaks around day 15 of pregnancy. This is consistent with there being a window of time during which endogenous *Notch*/*Rbpj* signaling is required to promote the development of alveolar/lobular structures. Thus, by the time the Wap promoter is active, endogenous *Notch*/*Rbpj* signaling has ceased.

In Wap-*Int3* female mammary glands, ductal development is normal but alveolar development does not occur (Gallahan *et al*., 1996). We interpret this to mean that target cells affected by WAP-*Int3*/*Rbpj* signaling must be alveolar committed progenitor cells downstream of those affected by endogenous *Notch*/*Rbpj* signaling. Thus, in the Wap-*Cre*/*Rbpj*$^{fl/fl}$/Wap-*Int3* females, loss of *Rbpj* allows mammary gland development to proceed normally. The effect of *Int3*/*Rbpj* signaling on mammary gland development is not unique to *Notch4/Int3*. Transgenic

mice containing either mouse MMTV-LTR-*Notch1-ICD* or mouse *Notch3-ICD* have mammary gland phenotypes that are very similar to that observed in MMTV LTR-*Int3* mice, namely mammary alveolar/lobular development is suppressed and mammary tumor development occurs (Hu *et al*., 2006). How does inappropriate *Notch*/*Rbpj* signaling block normal mammary gland development? One possibility is suggested by the work of Leong *et al*. (2007), who have shown that the transcriptional E-box binding repressor Slug is a direct target gene in the canonical *Notch*/*Rbpj* signaling pathway and that *Slug* expression leads to epithelial-to-mesenchymal transition by repressing the expression of E-cadherin. Mutations in the E-cadherin gene (*CDH1*) in breast cancer have been well documented (reviewed in Yoder *et al*., 2007). E-cadherin is involved in many cellular processes including morphogenesis, adhesion, recognition, communication and oncogenesis. Inactivation of its adhesive properties is often a key step in tumor progression and metastasis (reviewed by Bashyam, 2002).

The effect of Rbpj knockout on mammary tumorigenesis

Although deletion of *Rbpj* in the mammary gland suppresses the negative effect of *Int3* signaling on mammary alveolar development, it has little effect on the frequency of hyperproliferative lesions within individual mammary glands (average of 24 per gland), and also on the frequency of Int3-induced mammary tumors. In fact, 100% of the breeding Wap-*Int3*/*Rbpj* knockout females develop mammary tumors that could be transplanted in nude mice, although in each case, respectively, with a longer latency than the Wap-*Int3*/ *Rbpj* control tumors. The longer latency of primary and secondary tumor development in the Wap-*Int3*/ *Rbpj* knockout mice could be due to the fact that these glands fully develop and are more differentiated than the Wap-*Int3*/*Rbpj* control mammary glands. Similarly, *Notch*/*Rbpj*-induced *Slug* expression in MDA MB 231 tumor cells leads to epithelial-to-mesenchymal transition and confers on them the ability to form tumors in immunodeficient mice (Leong *et al*., 2007). Expression of a dominant negative mutant of *Rbpj* delayed but did not completely block tumor growth of the MDA-MB- 231 cells. Therefore, *Notch*/*Rbpj* signaling may be involved in the initiation of tumor development by sequestering or interacting with different transcriptional corepressors or activators or by regulating the expression of a different subset of target genes.

Immunohistochemical analysis of the primary and transplanted *Rbpj* knockout tumors for Neo, wild-type RBP-J and the targets of Notch signaling, Hes1 and Hey2, demonstrated that these tumors were negative for each of these proteins. This suggests that a minimum level of *Int3*/ *Rbpj* signaling is not required for the sustained growth of the primary or transplanted mammary tumors. However, our results cannot exclude the possibility that during the first pregnancy of the Wap-*Int3*/*Rbpj* knockout mice, there is a heterogeneity of cells in the mammary gland expressing Wap- *Cre* and WAP-*Int3*, and that in those cells not expressing Wap-*Cre*, as noted above, *Int3*/*Rbpj* signaling could be involved in the initiation of mammary tumorigenesis.

We have also examined the requirement for *Rbpj* expression on the ability of HC11 and HC11-*Int3* mammary epithelial cells to grow in soft agar. It is possible that the function of Int3 is simply to derepress RBP-J repressed genes and does not affect the activation of their transcription as suggested by Furriols and Bray (2001). Although the expression of several genes was derepressed in HC11 cells that were stably infected with vectors expressing *Rbpj* shRNA (unpublished data), the expression of these cellular genes did not confer on HC11 cells the capability to grow in soft agar. Furthermore, the stable expression of *Rbpj* shRNA in HC11-*Int3* cells did not affect their ability to grow in soft agar. In a related study, Stylianou *et al*. (2006) presented evidence that constitutively activated *Rbpj*- VP16 confers on normal human mammary MCF10A epithelial cells the ability to grow in soft agar, resistance to the induction of apoptosis and a reduction in E-cadherin expression. This is in contrast to our findings in which knockdown of *Rbpj* expression in HC11-*Int3* cells did not negatively affect their ability

to grow in soft agar. In addition, the level of apoptosis in the *Rbpj* knockout tumors was significantly lower than in the *Rbpj* control tumors. There are several aspects of these experiments that are difficult to evaluate. For instance, it is not known whether the chimeric activated Rbpj- VP16 protein possesses other novel properties that are not inherent to those exhibited by a wild-type Notch ICD/Rbpj interaction. It is also possible that the mechanism by which Notch1 ICD and Int3 induce mammary tumorigenesis is different, as the Notch1 ICD has a *trans*-activating domain C′ terminal to the ankyrin repeats that is missing in Int3.

Taken together, our data is most consistent with the concept that constitutive *Int3* signaling blocks mammary alveolar development through an *Rbpj*-dependent pathway and that *Int3*-induced mammary tumorigenesis or mammary tumor growth occurs as a consequence of *Int3* signaling that is not dependent on a canonical *Rbpj*-dependent pathway. Earlier reports have suggested that there are components of *Notch* signaling that occur independently of *Rbpj* and, in the case of Notch1, may be involved in neoplastic transformation (Shawber *et al*., 1996; Dumont *et al*., 2000; Jeffries and Capobianco, 2000; Levy *et al*., 2002; MacKenzie *et al*., 2004). In the literature, at least three additional binding partners for the Notch ICD have been reported: Deltex (Dtx) (luo *et al*., 2005), Hypoxia-induced factor-1α (Hif1α) (Zheng *et al*., 2008) and nuclear factor of κ light polypeptide gene enhancer in B-cells (Shin *et al*., 2006). Whether any one of these candidate binding partners or some as yet unknown binding partner collaborates with the Notch4 ICD to contribute to mammary tumorigenesis will be the subject of future studies.

Materials and methods

Mouse breeding and genotyping

We employed a mouse strain carrying a LoxP-flanked (floxed) *Rbpj* gene (*Rbpj*$^{flox/flox}$) provided by Dr Tasuku Honjo (Kyoto University, Kyoto, Japan), which has been described elsewhere (Han *et al*., 2002; Buono *et al*., 2006). To delete *Rbpj* in mammary epithelial cells *in vivo*, *Rbpj* $^{flox/flox}$ mice (Han *et al*., 2002) were bred with transgenic mice, provided by Dr Lothar Hennighausen (Laboratory of Genetics and Physiology, National Institute of Diabetes and Digestive and Kidney Diseases, National Institutes of Health, Bethesda, MD, USA), expressing Cre-recombinase under the control of the Wap promoter (Wagner *et al*., 1997) to generate mice having the genotype Wap-*Cre*$^{+}$/*Rbpj*$^{flox/flox}$ mice. Male Wap-*Cre*$^{+}$/*Rbpj*$^{flox/flox}$ mice were genetically crossed with female Wap-*Int3* mice (note, the Wap-*Int3* transgene is located on the X chromosome). Among the offspring were male mice having the genotype Wap-*Cre*$^{+}$/*Rbpj*$^{flox/+}$/WAP-*Int3*. These mice were genetically crossed with female Wap-*Cre*$^{+}$/*Rbpj*$^{flox/flox}$ mice. The offspring had the following genotypes: Wap-*Cre*$^{+}$/*Rbpj*$^{flox/flox}$/ Wap-*Int3* (designated as Wap-*Int3*/*Rbpj* knockout) and Wap- *Cre*$^{+}$/*Rbpj*$^{flox/+}$/ Wap-*Int3* (designated as Wap-*Int3*/*Rbpj* heterozygous) mice. The *Rbpj*$^{flox/flox}$/Wap-*Int3* mice, lacking the Wap-*Cre* transgene, were used as a control group and are referred to as Wap-*Int3*/*Rbpj* control mice. All the experimental mice had a mixed (129/C57BL/6/FVB) genetic background. The mice were treated according to the animal protocols approved by the Animal Care and Use Committee at National Institutes of Health.

Screening tail DNA for inheritance of the floxed *Rbpj* and Wap-*Int3* genes was performed by PCR as reported previously (Buono *et al*., 2006; Gallahan *et al*., 1996). Wap-*Cre* transgene was determined by PCR using the following primers: forward, 5′-CATCACTCGTTGCATCGACCGG-3′; and reverse, 5′-TA GAGCTGTGCCAGCCT CTTC-3′. DNAs were amplified for 34 cycles (94 °Cfor 30 s, 56 °Cfor 45 s and 72 °C for 1min).

Preparation of mammary tissue for analysis and transplantation

Mice were euthanized and mammary glands were examined grossly under a dissecting microscope. Mammary whole mounts and histology sections were prepared from the fourth abdominal gland as described previously (Raafat *et al*., 2004). Tumor tissue transplants were prepared as described previously (Raafat *et al*., 2007); briefly viable tissue from *Rbpj* control and knockout mammary tumors was transplanted into the inguinal mammary glands of 10-week-old recipients (homozygous athymic NCR-nu females). All the recipients were kept as nulliparous mice and were palpated twice weekly. Experiments were repeated at least twice, and at least five mice were used in each experiment.

Immunohistochemistry

Immunohistochemical analysis was carried out as described previously (Raafat *et al*., 2007). Primary antibodies were diluted: 500×; β-casein (SC-30042), 200X; Hes-1 (SC-25392), 200X; Hey-2 (Protein Tech Group, Inc-10597-1-AP), 200X; Neo (USBiological-N2008-05), 500X; and Rbpj (SC-8213), 500×, PCNA (sc-9857), 100×, in phosphate-buffered saline–1% bovine serum albumin. Appropriate biotinylated secondary anti-goat (PK-6105, Vector Laboratories Inc., Burlingame, CA, USA) or anti-rabbit (PK-6101, Vector Laboratories Inc., Burlingame, CA, USA) antibodies were diluted according to the manufacturer's recommendations. For apoptosis, the Roche *in situ* cell detection POD kit (1684817, Roche, Indianapolis, IN, USA) was used according to the manufacturer's recommendations. Labeling index was determined in at least a total of 3000 cells in each experimental condition.

Lentivirus production and transduction, proliferation and colony growth in soft agar

HEK293T/17 cells were purchased from the ATCC (Mannassas, VA, USA) and grown in DMEM, supplemented with 10% fetal bovine serum and Pen/Strep (Invitrogen; Carlsbad, CA, USA). A shRNA knockdown vector for murine *Rbpj*, derived from the RNAi consortium, was purchased from Open Biosystems Inc. (Huntsville, AL, USA). Purchased Clone ID numbers included TRCN0000097284–88 and were designated as H2 through H6, respectively. A control vector expressing the nontarget shRNA sequence (CCGGCAACAAGATGAA GAGCACCAACTCGAGTTGGTGCTCTTCATCTTGTTG TTTTT) was purchased from Sigma-Aldrich (St Louis, MO, USA). The lentiviral helper plasmids, psPax2 and pMD2.G, were purchased from Addgene (Cambridge, MA, USA). All viral work conformed to accepted Biosafety Level 2+ guidelines as described by the National Institutes of Health (http://bmbl.od.nih.gov/contents.htm). Briefly, knockdown vectors (H2–H6) were cotransfected with helper plasmids (psPax2 and pMD2.G) in a ratio of 10:7.5:3, respectively, in HEK293T/17, using FugeneHD (Roche Applied Science; Indianapolis, IN, USA). HC11 mouse mammary epithelial cells were transduced with lentiviral particles at approximately 40% confluence for 8–12 h followed by replacement with fresh media. Cells were selected for puromycin (4.5 mg/ml, Sigma- Aldrich, St Louis, MO, USA) resistance 36 h post-infection. For proliferation, cells were plated at a density of 1×10^3 per well in 24-well plates in regular growing media (day 0). The number of cells was determined every day until confluence using a Coulter counter.

The proliferation ratios were calculated from the initial start point (day 0) and the data presented are the mean of three independent experiments. Soft agar colony growth was conducted as described previously (Raafat *et al*., 2007). Colonies measuring 0.2 μm or larger were counted using the AccuCount 1000 colony counter (Biologics Inc., Manassas, VA, USA).

Statistics

Quantitative values are represented as the mean of at least three experiments. All *in vivo* experiments were repeated at least three times, and at least five mice were used in each

experiment. The statistical significance of the difference between groups was determined by the Wilcoxon rank sum test. Comparisons resulting in *P*-values less than 0.05 were considered as statistically significant and identified in the figures with an asterisk (*).

Acknowledgments

The *Rbpj*$^{flox/flox}$ mice were kindly provided by Dr Tasuku Honjo, Department of Medical Chemistry, Graduate School of Medicine, Kyoto University, Kyoto, Japan, and the WAP-*Cre* mice were kindly provided by Dr Lothar Hennighausen, Laboratory of Genetics and Physiology, National Institute of Diabetes and Digestive and Kidney Diseases, National Institutes of Health, Bethesda, MD, USA. This research was supported by the Intramural Research Program of the NIH, National Cancer Institute, Center for Cancer Research.

References

Bashyam MD. Understanding cancer metastasis: an urgent need for using differential gene expression analysis. Cancer 2002;94:1821–1829. [PubMed: 11920546]

Bray S, Furriols M. Notch pathway: making sense of suppressor of hairless. Curr Biol 2001;11:R217–R221. [PubMed: 11301266]

Buono KD, Robinson GW, Martin C, Shi S, Stanley P, Tanigaki K, et al. The canonical Notch/RBP-J signaling pathway controls the balance of cell lineages in mammary epithelium during pregnancy. Dev Biol 2006;293:565–580. [PubMed: 16581056]

Callahan R, Egan SE. Notch signaling in mammary development and oncogenesis. J Mammary Gland Biol Neoplasia 2004;9:145–163. [PubMed: 15300010]

Dumont E, Fuchs KP, Bommer G, Christoph B, Kremmer E, Kempkes B. Neoplastic transformation by Notch is independent of transcriptional activation by RBP-J signalling. Oncogene 2000;19:556–561. [PubMed: 10698525]

Furriols M, Bray S. Dissecting the mechanisms of suppressor of hairless function. Dev Biol 2000;227:520–532. [PubMed: 11071771]

Furriols M, Bray S. A model Notch response element detects Suppressor of Hairless-dependent molecular switch. Curr Biol 2001;11:60–64. [PubMed: 11166182]

Gallahan D, Callahan R. Mammary tumorigenesis in feral mice: identification of a new int locus in mouse mammary tumor virus (Czech II)-induced mammary tumors. J Virol 1987;61:66–74. [PubMed: 3023708]

Gallahan D, Callahan R. The mouse mammary tumor associated gene INT3 is a unique member of the NOTCH gene family (NOTCH4). Oncogene 1997;14:1883–1890. [PubMed: 9150355]

Gallahan D, Jhappan C, Robinson G, Hennighausen L, Sharp R, Kordon E, et al. Expression of a truncated Int3 gene in developing secretory mammary epithelium specifically retards lobular differentiation resulting in tumorigenesis. Cancer Res 1996;56:1775–1785. [PubMed: 8620493]

Han H, Tanigaki K, Yamamoto N, Kuroda K, Yoshimoto M, Nakahata T, et al. Inducible gene knockout of transcription factor recombination signal binding protein-J reveals its essential role in T versus B lineage decision. Int Immunol 2002;14:637–645. [PubMed: 12039915]

Hu C, Dievart A, Lupien M, Calvo E, Tremblay G, Jolicoeur P. Overexpression of activated murine Notch1 and Notch3 in transgenic mice blocks mammary gland development and induces mammary tumors. Am J Pathol 2006;168:973–990. [PubMed: 16507912]

Imatani A, Callahan R. Identification of a novel NOTCH-4/ INT-3 RNA species encoding an activated gene product in certain human tumor cell lines. Oncogene 2000;19:223–231. [PubMed: 10645000]

Jeffries S, Capobianco AJ. Neoplastic transformation by Notch requires nuclear localization. Mol Cell Biol 2000;20:3928–3941. [PubMed: 10805736]

Jhappan C, Gallahan D, Stahle C, Chu E, Smith GH, Merlino G, et al. Expression of an activated Notch-related int-3 transgene interferes with cell differentiation and induces neoplastic transformation in mammary and salivary glands. Genes Dev 1992;6:345–355. [PubMed: 1372276]

Kato H, Sakai T, Tamura K, Minoguchi S, Shirayoshi Y, Hamada Y, et al. Functional conservation of mouse Notch receptor family members. FEBS Lett 1996;395:221–224. [PubMed: 8898100]

Kordon EC, Smith GH, Callahan R, Gallahan D. A novel non-mouse mammary tumor virus activation of the Int-3 gene in a spontaneous mouse mammary tumor. J Virol 1995;69:8066–8069. [PubMed: 7494323]

Leong KG, Niessen K, Kulic I, Raouf A, Eaves C, Pollet I, et al. Jagged1-mediated Notch activation induces epithelial-to-mesenchymal transition through Slug-induced repression of E-cadherin. J Exp Med 2007;204:2935–2948. [PubMed: 17984306]

Levy OA, Lah JJ, Levey AI. Notch signaling inhibits PC12 cell neurite outgrowth via RBP-J-dependent and -independent mechanisms. Dev Neurosci 2002;24:79–88. [PubMed: 12145413]

Luo D, Renault VM, Rando TA. The regulation of Notch signaling in muscle stem cell activation and postnatal myogenesis. Semin Cell Dev Biol 2005;16:612–622. [PubMed: 16087370]

MacKenzie F, Duriez P, Wong F, Noseda M, Karsan A. Notch4 inhibits endothelial apoptosis via RBP-J kappa-dependent and -independent pathways. J Biol Chem 2004;279:11657–11663. [PubMed: 14701863]

Oakes SR, Hilton HN, Ormandy CJ. The alveolar switch: coordinating the proliferative cues and cell fate decisions that drive the formation of lobuloalveoli from ductal epithelium. Breast Cancer Res 2006;8:207. [PubMed: 16677418]

Raafat A, Bargo S, Anver MR, Callahan R. Mammary development and tumorigenesis in mice expressing a truncated human Notch4/Int3 intracellular domain (h-Int3sh). Oncogene 2004;23:9401–9407. [PubMed: 15531924]

Raafat A, Zoltan-Jones A, Strizzi L, Bargo S, Kimura K, Salomon D, et al. Kit and PDGFR-alpha activities are necessary for Notch4/Int3-induced tumorigenesis. Oncogene 2007;26:662–672. [PubMed: 16878155]

Robbins J, Blondel BJ, Gallahan D, Callahan R. Mouse mammary tumor gene int-3: a member of the notch gene family transforms mammary epithelial cells. J Virol 1992;66:2594–2599. [PubMed: 1312643]

Shawber C, Nofziger D, Hsieh JJ, Lindsell C, Bögler O, Hayward D, et al. Notch signaling inhibits muscle cell differentiation through a CBF1-independent pathway. Development 1996;122:3765–3773. [PubMed: 9012498]

Shin HM, Minter LM, Cho OH, Gottipati S, Fauq AH, Golde TE, et al. Notch1 augments NF-kappaB activity by facilitating its nuclear retention. EMBO J 2006;25:129–138. [PubMed: 16319921]

Smith GH, Gallahan D, Diella F, Jhappan C, Merlino G, Callahan R. Constitutive expression of a truncated INT3 gene in mouse mammary epithelium impairs differentiation and functional development. Cell Growth Differ 1995;6:563–577. [PubMed: 7544153]

Stylianou S, Clarke RB, Brennan K. Aberrant activation of notch signaling in human breast cancer. Cancer Res 2006;66:1517–1525. [PubMed: 16452208]

Wagner KU, Wall RJ, St-Onge L, Gruss P, Wynshaw-Boris A, Garrett L, et al. Cre-mediated gene deletion in the mammary gland. Nucleic Acids Res 1997;25:4323–4330. [PubMed: 9336464]

Yoder BJ, Wilkinson EJ, Massoll NA. Molecular and morphologic distinctions between infiltrating ductal and lobular carcinoma of the breast. Breast J 2007;13:172–179. [PubMed: 17319859]

Zheng X, Linke S, Dias JM, Gradin K, Wallis TP, Hamilton BR, et al. Interaction with factor inhibiting HIF-1 defines an additional mode of cross-coupling between the Notch and hypoxia signaling pathways. Proc Natl Acad Sci USA 2008;105:3368–3373. [PubMed: 18299578]

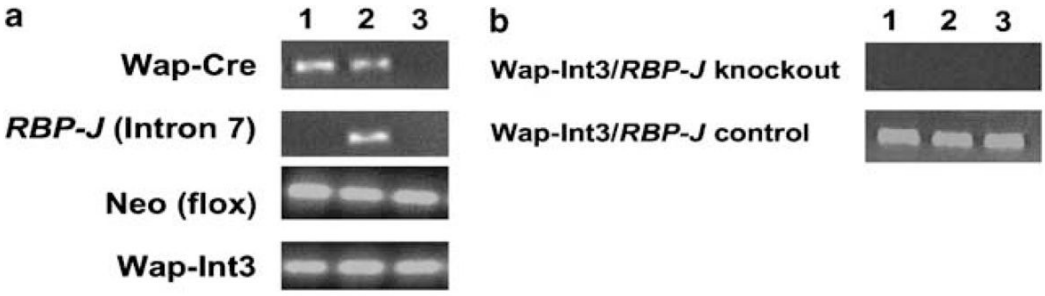

Figure 1.

Genotyping and analysis of mice. Wap-*Cre*/*Rbpj*$^{flox/flox}$ mice were genetically crossed with Wap-*Cre*/ *Rbpj*$^{+/flox}$/Wap-Int3 mice, to generate Wap-*Cre*$^{+}$/*Rbpj*$^{flox/flox}$/Wap-*Int3* (Wap-*Int3*/*Rbpj* knockout), Wap-*Cre*$^{+}$/*Rbpj*$^{flox/+}$/Wap-*Int3* (Wap-*Int3*/*Rbpj* heterozygous) and *Rbpj*$^{flox/flox}$/Wap-*Int3* (Wap-*Int3*/*Rbpj* control) mice, as described in the Materials and methods. (**a**) PCR tail DNA analysis of Wap-*Cre*/*Rbpj* $^{-/-}$/Wap-*Int3* (lane 1), Wap-*Cre*/ *Rbpj*$^{-/+}$/Wap-*Int3* (lane 2) and *Rbpj*$^{flox/flox}$/Wap-*Int3* (lane 3, note that because of the large size of the neomycin phosphotransferase cassette inserted in *Rbpj* intron 7, Wap-*Int3*/*Rbpj* control mice test negative for *Rbpj* in the tail DNA analysis). (**b**) *Neo* RT–PCR analysis of total RNA extracted from three each of Wap-*Int3*/*Rbpj* knockout and Wap-*Int3*/*Rbpj* control tumors. Only the Wap-*Int3*/*Rbpj* knockout tumor RNAs are negative for *Neo*. RT–PCR, reverse transcriptase PCR.

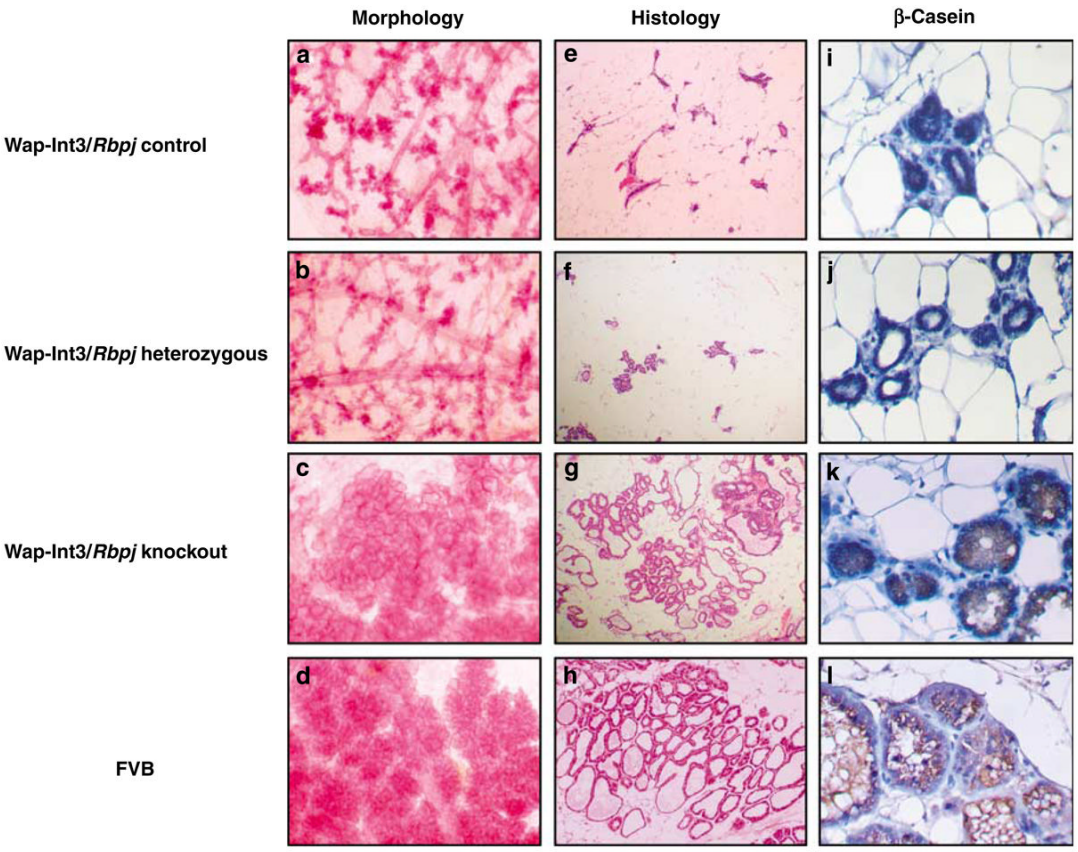

Figure 2.

Morphology, histology and immunohistochemical analysis of Wap-Int3/RBP-J knockout mammary glands. Photomicrographs of mammary gland wholemounts (**a**–**d**); histological sections (**e**–**h**); and β-casein immunohistochemistry (**i**–**l**) in the Wap-*Int3*/ *Rbpj* control (panels **a**, **e**, and **i**), Wap-*Int3*/*Rbpj* heterozygous (panels **b**, **f** and **j**), Wap-*Int3*/*Rbpj* knockout (panels **c**, **g** and **k**) and FVB (**d**, **h** and **l**) mice collected from the number 4 inguinal mammary gland from day 1 lactating mice. Of the experimental mice, only the Wap-*Int3*/*Rbpj* knockout mice were able to lactate, showed normal alveolar development (**c**, **g**) and were positive for the milk protein, β-casein (**k**), confirming the morphological and histological observations. Panels **a**–**h** are at ×10 original magnification and panels **i**–**l** are at ×40 original magnification. Each treatment group contained at least 10 mice.

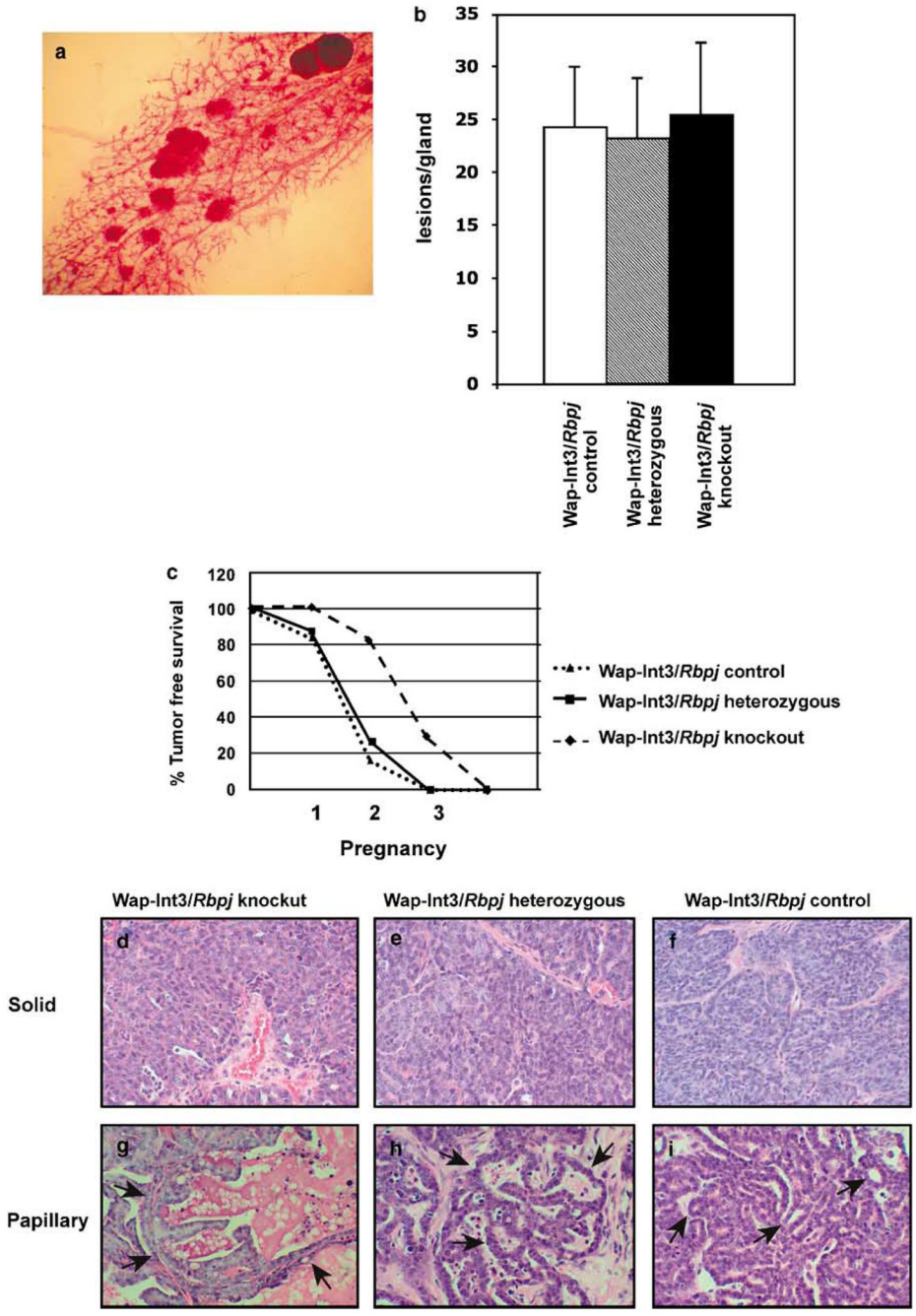

Figure 3.

Mammary gland lesions, overall tumor-free survival and tumor histological analysis. (**a**) A representative wholemount from Wap-*Int3*/*Rbpj* knockout mouse showing several hyperproliferative lesions in the mammary gland; (**b**) the frequency of hyperproliferative lesions in Wap-*Int3*/*Rbpj* knockout, Wap-*Int3*/*Rbpj* heterozygous and Wap-*Int3*/*Rbpj* control mice in the fourth inguinal mammary gland, after the second parity; (**c**) the overall tumor-free survival of Wap-*Int3*/*Rbpj* control, Wap-*Int3*/*Rbpj* heterozygous and Wap-*Int3*/*Rbpj* knockout mice; histopathology of solid mammary adenocarcinomas from (**d**) Wap-*Int3*/*Rbpj* knockout tumor, (**e**) Wap-*Int3*/*Rbpj* heterozygous tumor, and (**f**) Wap-*Int3*/*Rbpj* control tumor; and (**g**) a papillary adenocarcinoma from Wap-*Int3*/*Rbpj* knockout mouse, (**h**) a Wap-*Int3*/*Rbpj*

heterozygous tumor and (**i**) a Wap-*Int3*/*Rbpj* control tumor. All figures were hematoxylin-and-eosin-stained and are at ×40 original magnification.

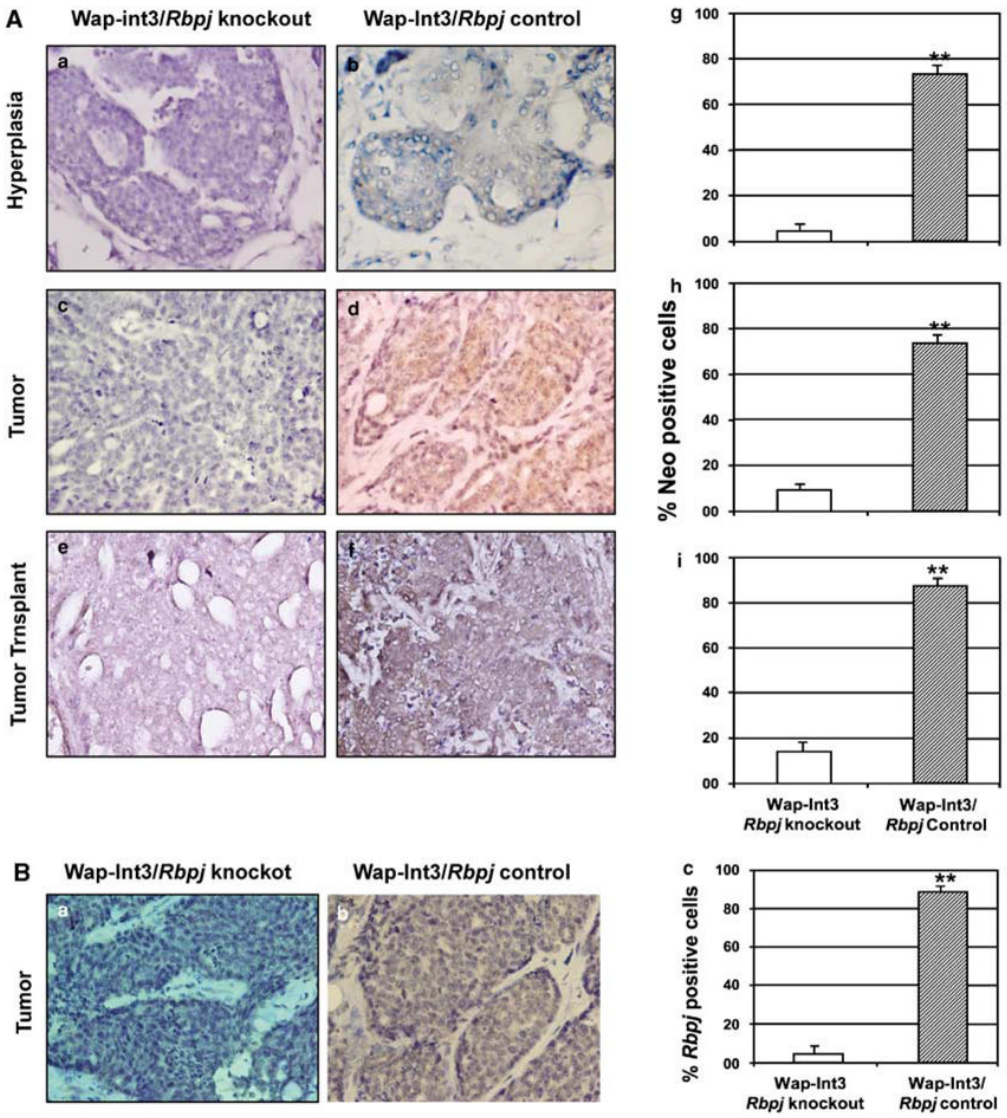

Figure 4.

Photomicrographs of immunohistochemical staining of Neo and Rbpj in Wap-*Int3*/*Rbpj* knockout hyperplasia, primary mammary tumor and transplanted mammary tumor. (**A**) IHC analysis of Neo in Wap-*Int3*/*Rbpj* knockout (a, c and e) and Wap-*Int3*/ *Rbpj* control (b, d and f) hyperplasia (a, b), primary tumor (c, d) and tumor transplants (e, f). Only Wap-*Int3*/*Rbpj* control tissue was positive for Neo. Positive cells were scored in the hyperplasia (g), tumor (h) and mammary transplants (i) and labeling index was expressed as a percentage of positive nuclei of 3000 counted cells. In all tissues, neomycin phosphotransferse was significantly lower in $Rbpj^{-/-}$/Wap-*Int3* than $Rbpj^{-/+}$/Wap-*Int3*. (**B**) IHC analysis of Rbpj using an antibody that recognizes the C′-terminal end of the protein (that is, wild-type protein) in a Wap-*Int3*/*Rbpj* knockout tumor (a) and Wap-*Int3*/*Rbpj* control tumor (b). Positive cells were scored in each and labeling index expressed as a percentage of positive nuclei of 3000 counted cells (**c**). A total of at least 5–6 mice were used for each experiment. **P*<0.05. Original magnification was at ×40. IHC, immunohistochemistry.

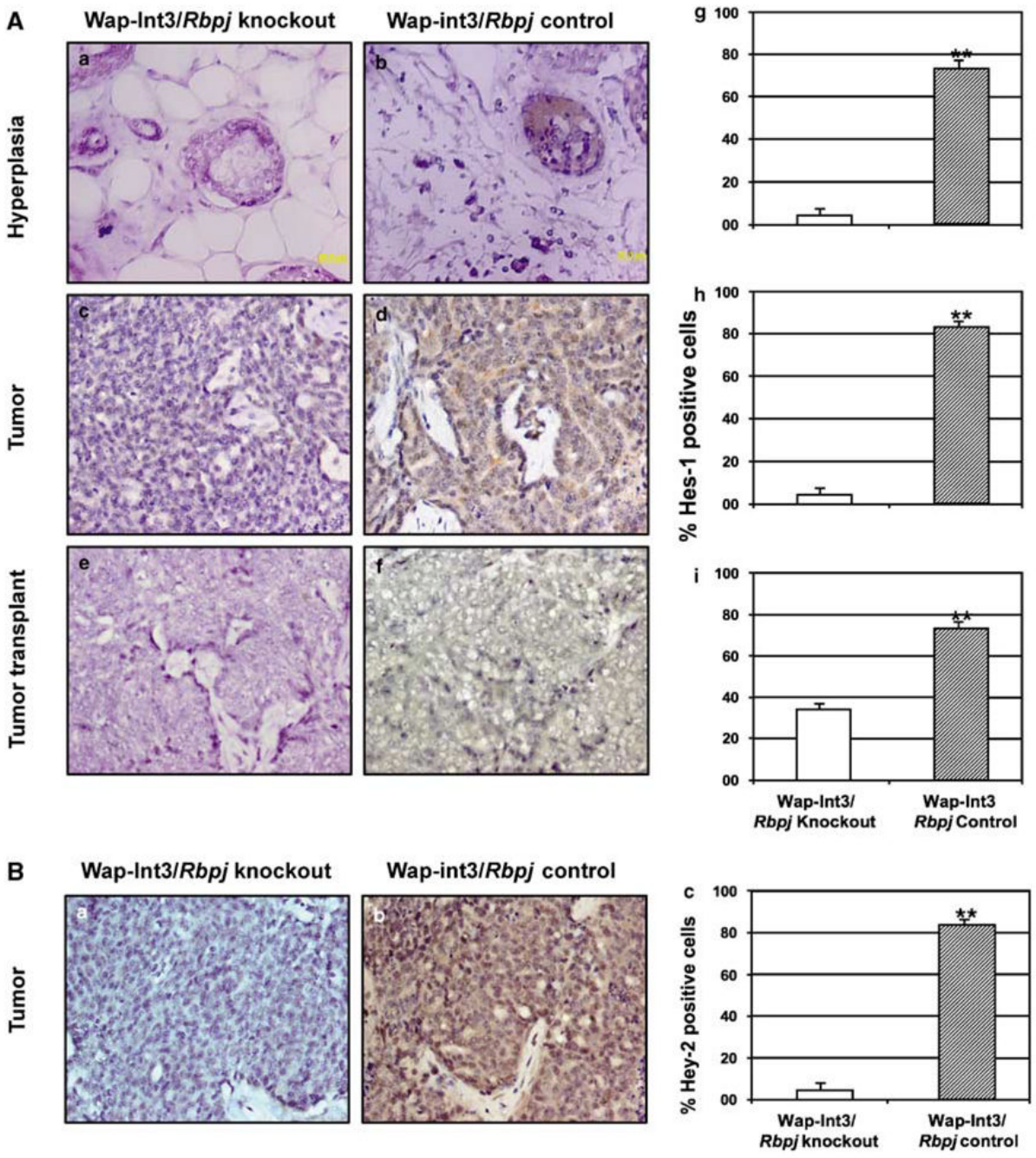

Figure 5.

Photomicrographs of immunohistochemical staining of Hes1 and Hey2 in Wap-*Int3*/*Rbpj* knockout hyperplasia, primary mammary tumor and transplanted mammary tumor. (**A**) IHC analysis of Hes-1 in Wap-*Int3*/*Rbpj* knockout (a, c and e) and Wap-*Int3*/ *Rbpj* control (b, d and f) hyperplasia (a, b), primary tumor (c, d) and transplanted tumor (e, f). Only Wap-*Int3*/*Rbpj* control tissue was positive for Hes-1. Positive cells were scored in the hyperplasia (g), tumor (h) and transplanted tumor (i) and labeling index was expressed as a percentage of positive nuclei of at least 3000 counted cells. In all tissues, Hes-1 was significantly lower in Wap-*Int3*/*Rbpj* knockout than Wap-*Int3*/*Rbpj* control. (**B**) IHC analysis of Hey2 in a Wap-*Int3*/ *Rbpj* knockout tumor (a) and Wap-*Int3*/*Rbpj* control tumor (b). Positive cells were scored in

each, and labeling index was expressed as a percentage of positive nuclei of 3000 counted cells (c). Hey2 was detected only in the Wap-*Int3*/*Rbpj* control tumor. A total of 5–6 mice were used for each experiment. **P*<0.05. Original magnification was at ×40. IHC, immunohistochemistry.

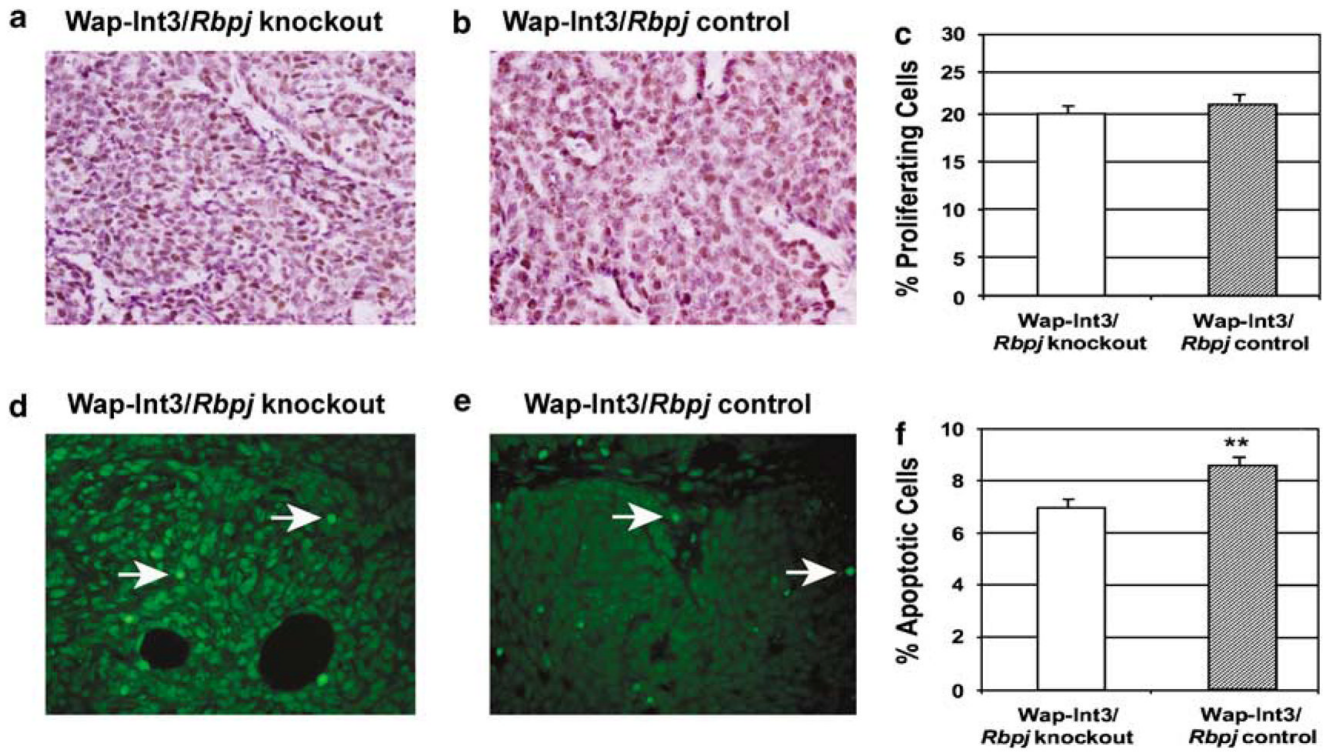

Figure 6.

In vivo effect of *Rbpj* deletion on proliferation and apoptosis of WAP-*Int3*/*Rbpj* knockout and control mammary tumors. WAP-*Int3*/*Rbpj* knockout (**a** and **d**) and control (**b** and **e**) tumor-bearing mice were euthanized and mammary tumor tissue was collected and processed for proliferation (**a** and **b**) and apoptosis (**d** and **e**) as described in the Materials and methods. Deletion of *Rbpj* in the WAP-*Int3* mice did not affect the tumor proliferation; however, apoptosis was significantly higher in the WAP-*Int3*/*Rbpj* knockout mammary tumors than in the WAP-*Int3*/*Rbpj* control tumors. The proliferating and apoptotic cells were scored, and labeling index was expressed as a percentage of positive nuclei of at least 3000 counted cells. A total of at least 5–6 mice were used for each experiment. Arrows point to apoptotic cells. **P*<0.05. Original magnification was at ×40.

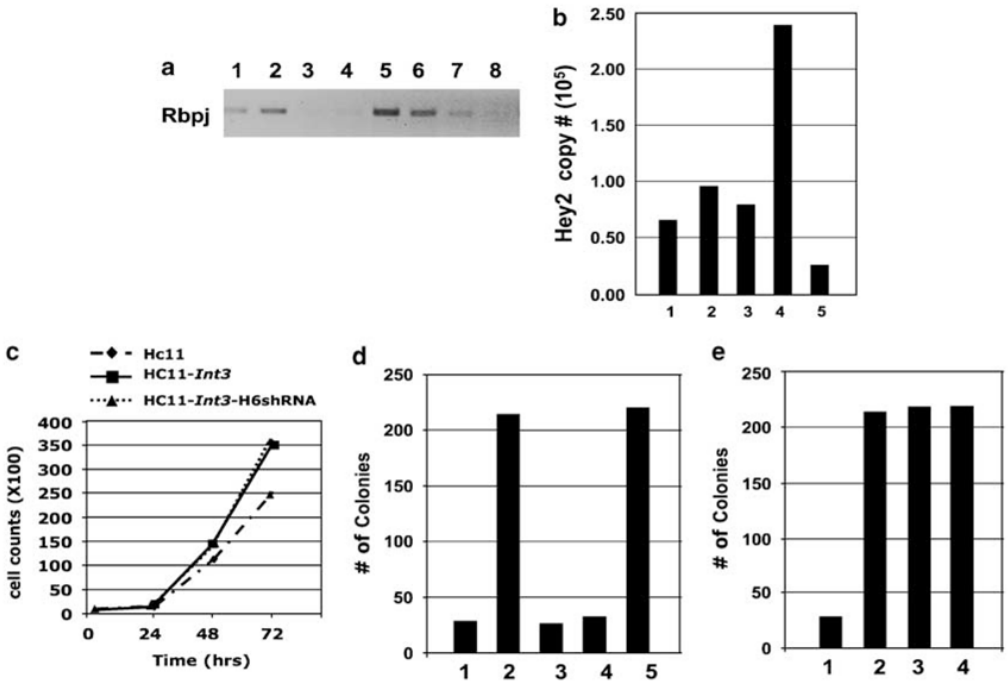

Figure 7.

Is *Rbpj* necessary for anchorage-independent growth of HC11 and HC11-*Int3* cells in soft agar? HC11 and HC11-*Int3* cells stably expressing *Rbpj* shRNA (HC11-H5shRNA, HC11-H6shRNA, HC11-*Int3*-H5shRNA, and HC11-*Int3*-H6shRNA) were tested for the expression of *Rbpj* RNA by RT–PCR (**a**), effect of *Rbpj* shRNA on Notch signaling (**b**) and proliferation (**c**) and for their ability to grow in soft agar (**d** and **e**). (**a**) HC11 (lane 1), HC11+scrambled vector (lane 2), HC11+*Rbpj*H5shRNA (lane 3), HC11+*Rbpj*H6shRNA (lane 4), HC11-*int3* (lane 5), HC11-*Int3*+scrambled vector (lane 6), HC11-*Int3*+*Rbpj*H5shRNA (lane 7) and HC11-*Int3*+*Rbpj*H6shRNA (lane 8). *Rbpj*H5 and H6shRNA both blocked *Rbpj* expression (Lanes 3, 4, 7 and 8), but *Rbpj*H6shRNA was more efficient. (**b**) Quantitative RT–PCR analysis of *Hey2* mRNA in the HC-11 (lane 1), HC11+ scrambled vector (lane 2), HC11+scrambled vector + *Rbpj* H6shRNA (lane 3), Hc11+*Int3* (lane 4), Hc11+*Int3*+*Rbpj*H6shRNA (lane 5). *Rbpj* H6shRNA blocked Notch signaling (lane 4 vs lane 5). (**c**) Growth curves for HC11, HC11-Int3 and HC11-*Int3*-H6shRNA mammary epithelial cells. The rate of proliferation of HC11-Int3 and HC11-Int3 cells stably expressing *Rbpj* H6shRNA was not significantly different. (**d**) 15 000 cells were seeded in soft agar in the presence and absence of *Rbpj* H6shRNA. HC11 (lane 1), HC11- *Int3* (lane 2), HC11+scrambled vector (lane 3), HC11+*Rbpj* H6shRNA (lane 4) and HC11-*Int3*+scrambled vector (lane 5). HC11 cells did not acquire the ability to grow in soft agar in the absence of *Rbpj* (lanes 4 and 5). (**e**) Soft agar growth of 15 000 HC11-*Int3* cells in the presence and absence of *Rbpj* H6shRNA. HC11 (lane 1), HC11-*Int3* (lane 2), HC11-*Int3*+scrambled vector (lane 3), HC11- Int3+*Rbpj* H6shRNA (lane 4). HC11-*Int3* cells did not lose the ability to grow in soft agar in the absence of *Rbpj* (Lane 4). RT–PCR, reverse transcriptase PCR.